

Cuprizone intoxication induces cell intrinsic alterations in oligodendrocyte metabolism independent of copper chelation

Alexandra Taraboletti¹, Tia Walker³, Robin Avila⁴, He Huang¹, Joel Caporoso⁵, Erendra Manandhar¹, Thomas C. Leeper⁶, David Modarelli¹, Satish Medicetty⁴, and Leah P. Shriver^{1,2*}

¹Department of Chemistry, University of Akron, Akron, OH 44325

²Department of Biology, University of Akron, Akron, OH 44325

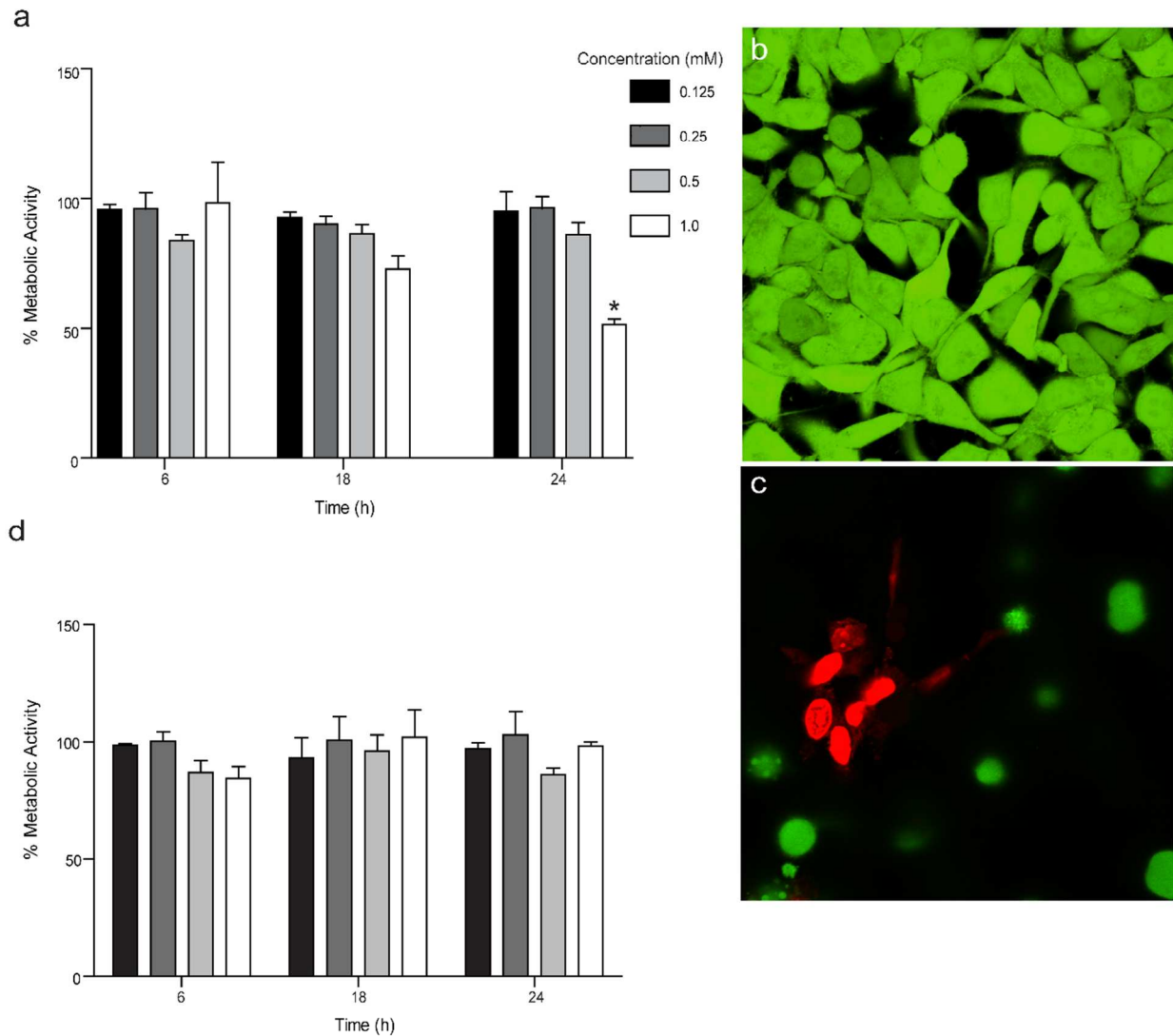
³Department of Chemistry, Indiana University Northwest, Gary, IN 46408

⁴Renovo Neural, Inc. Cleveland, OH 44106

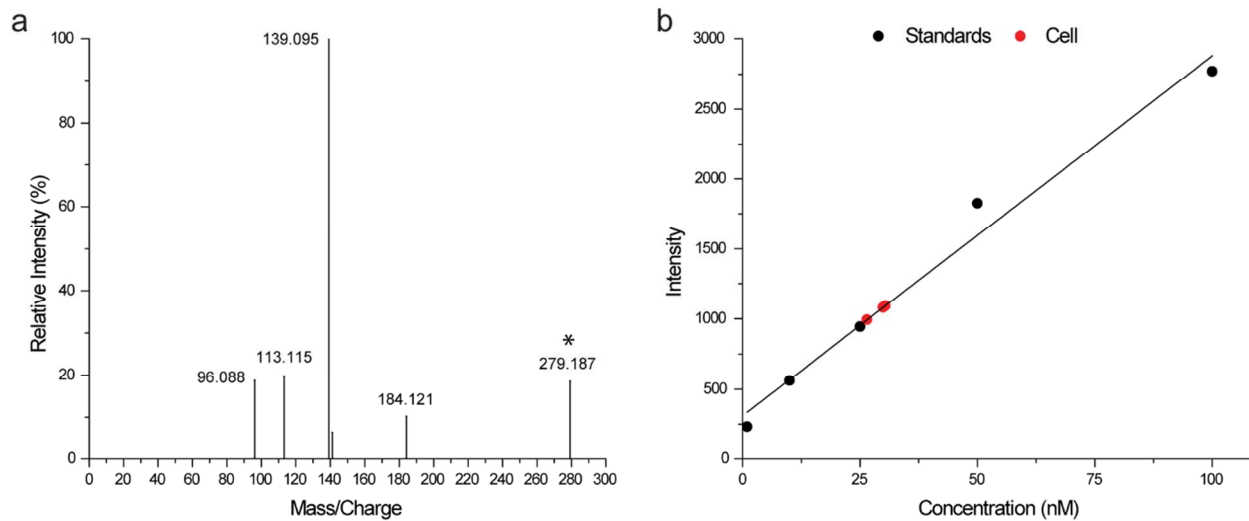
⁵Department of Anesthesiology, University of Pittsburgh School of Medicine, Pittsburgh, PA 15260

⁶Department of Chemistry, College of Wooster, Wooster, OH 44691

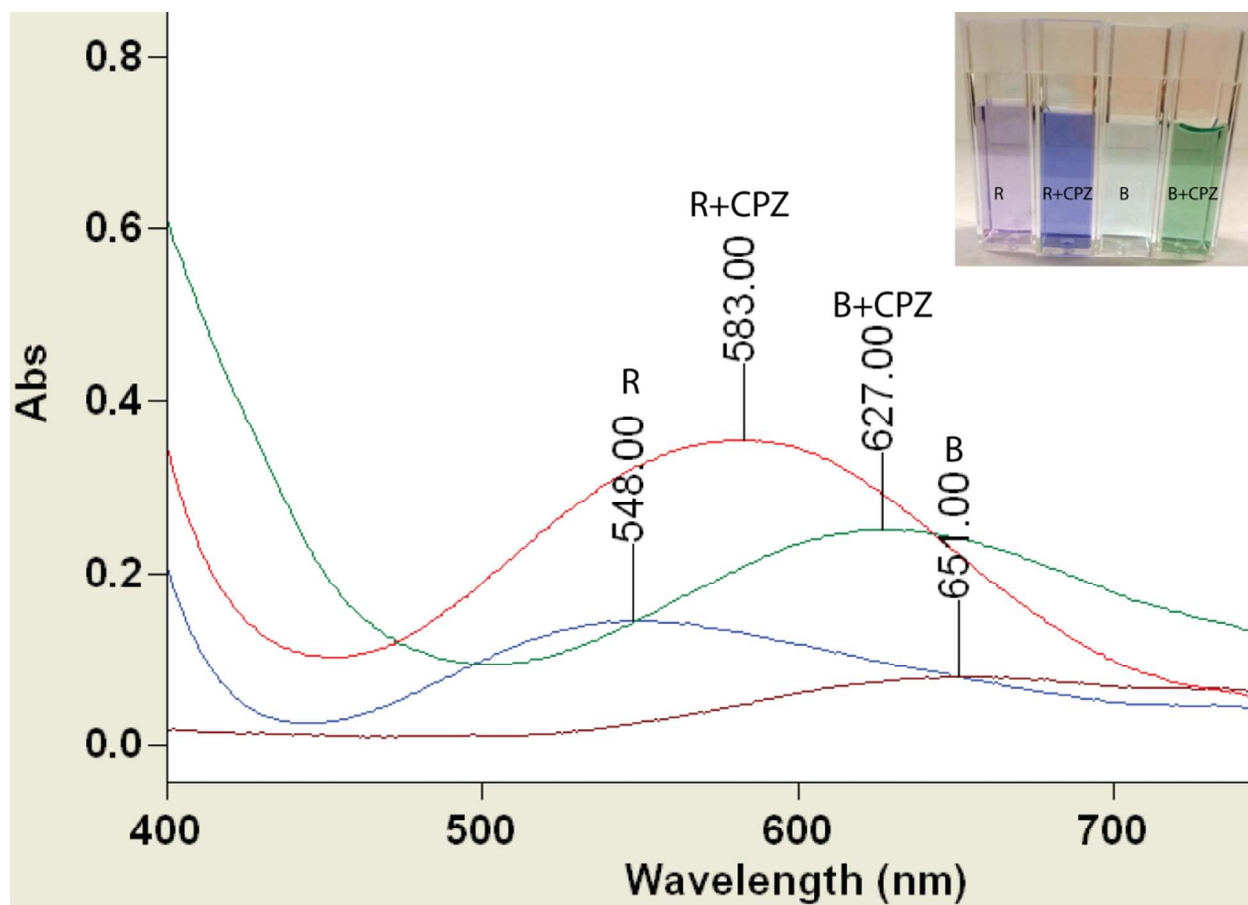
Supplemental Information



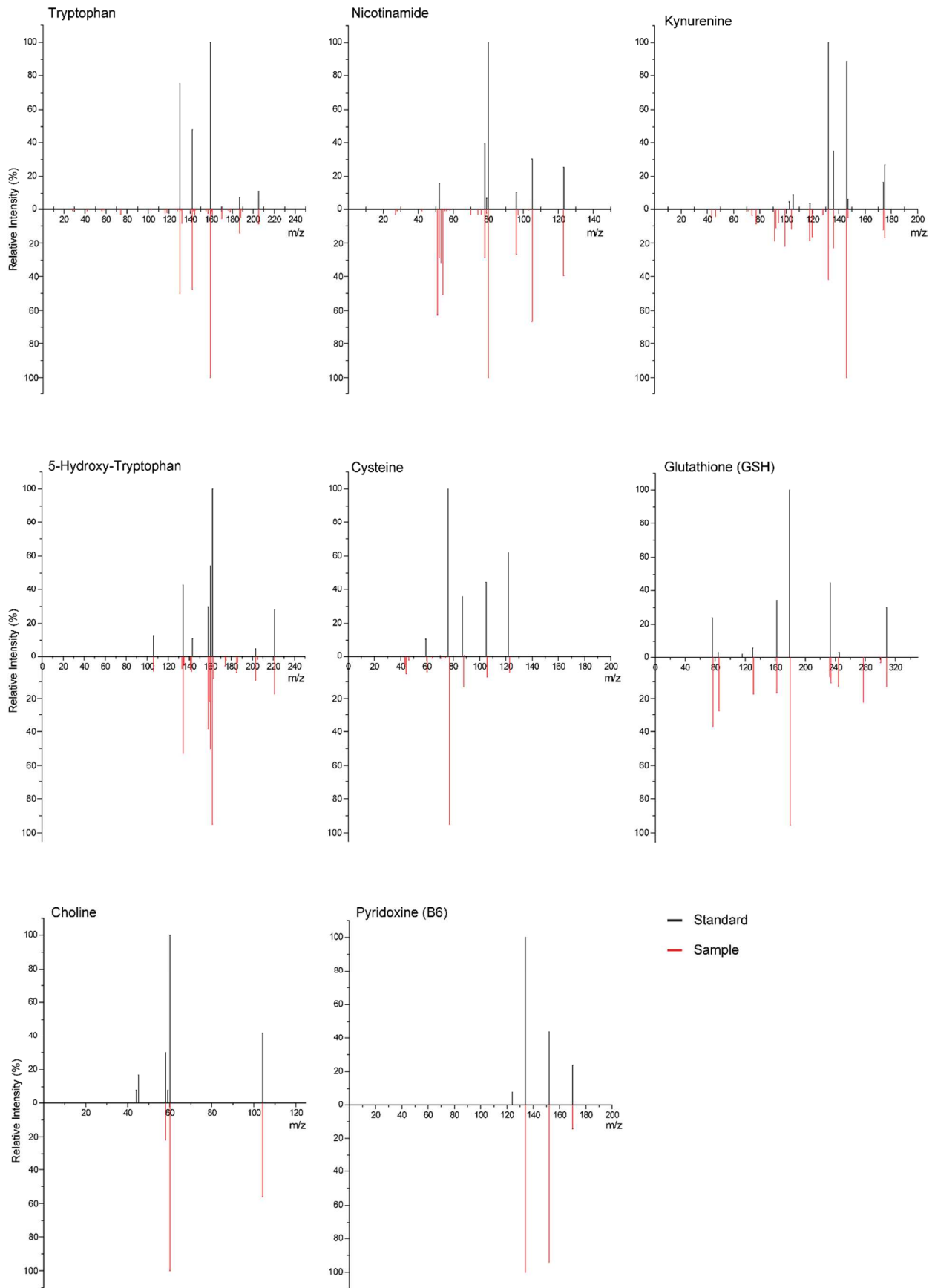
Supplemental Figure 1: Oligodendrocyte cells show changes in metabolic activity after cuprizone treatment while a rat astrocyte cell line does not. (a) An MTT assay was used to measure the metabolic activity of the MO3.13 cells treated with increasing concentrations of CPZ at 6, 18, and 24 hours. Concentrations ranged from 0.125 μ M to 1 mM (black to white) (n=12 cultures per concentration per time point). Percent activity was compared to vehicle-treated cells. Live cell fluorescence microscopy of MO3.13 cell (100X) treated with vehicle (b) or 1mM CPZ (c) and stained with 2 μ M calcein AM (green) and 4 μ M EthD-1 (red) after 12 hours of treatment. (d) Metabolic Activity measured by MTT assay in a rat astrocyte cell line (DI TNC1) treated with increasing concentrations of CPZ at 6, 18, and 24 hours. Concentrations ranged from 0.125 μ M to 1 mM (black to white) (n=12 cultures per concentration per time point).



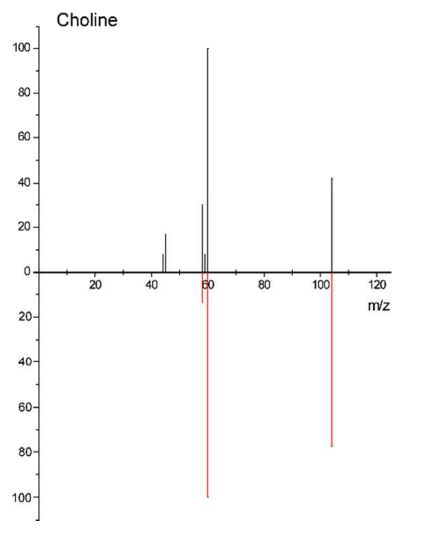
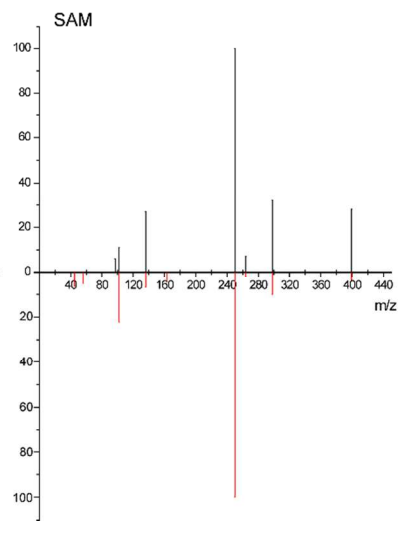
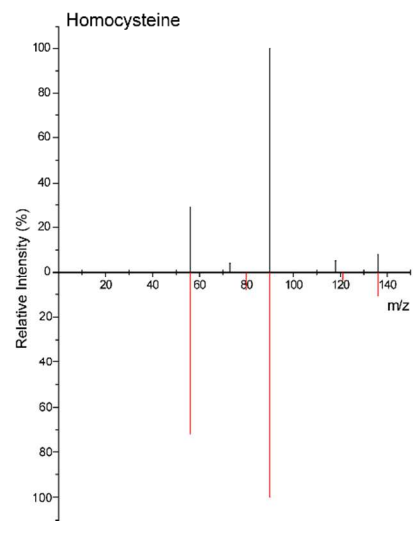
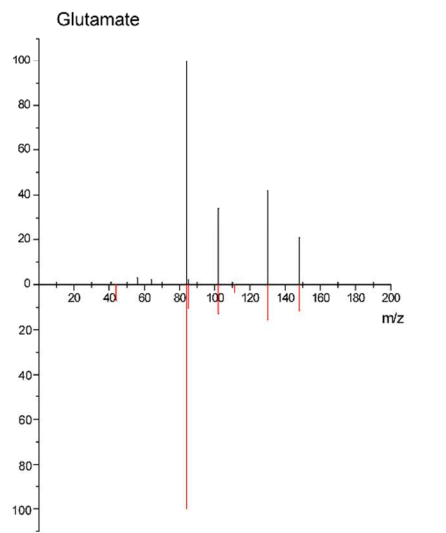
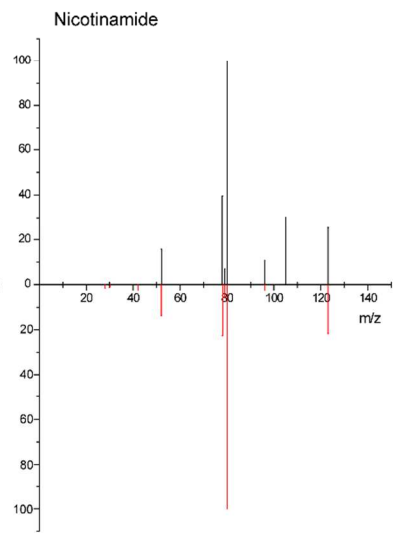
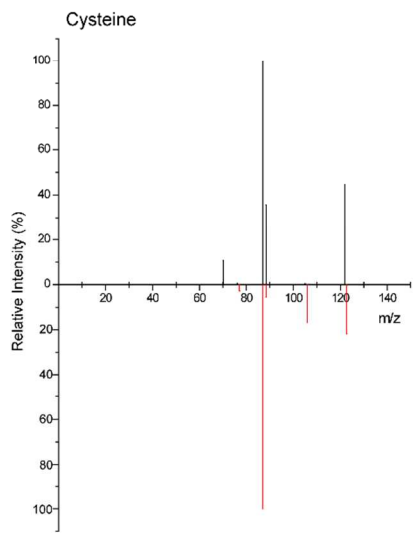
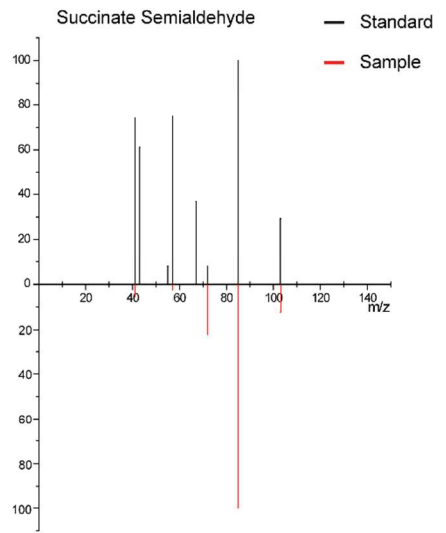
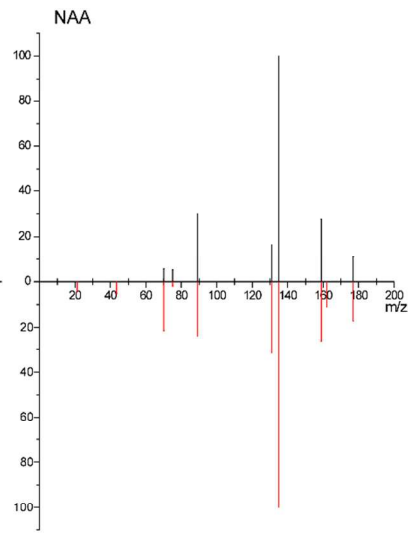
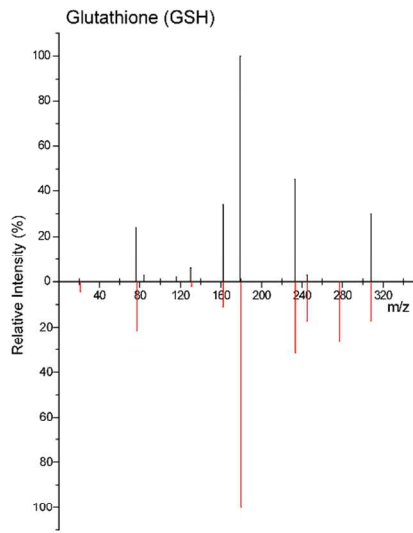
Supplemental Figure 2: Determination of CPZ uptake in cells by mass spectrometry. (a) MS/MS data for unbound CPZ (* parent ion) (b) The standard curve for CPZ concentrations from 1 to 100 nM. Levels in cells are shown in red. The transition m/z 279.18 \rightarrow m/z 139.09 was used to determine concentration in cells.

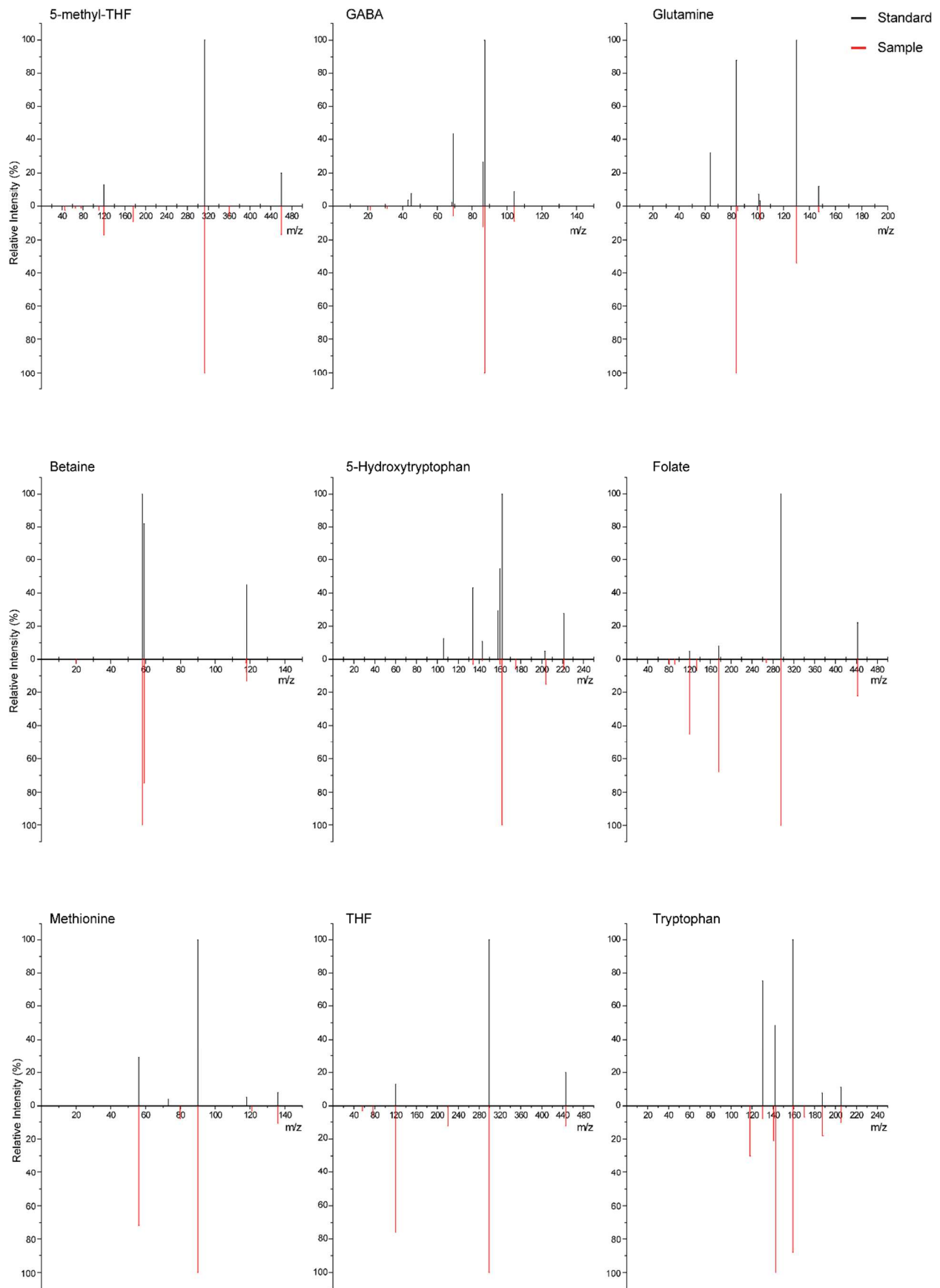


Supplemental Figure 3: Absorbance shifts induced by CPZ addition to copper active site mimics. Absorbance spectra and colored photograph (inset) of both mimics ("R" and "B") when dissolved in water at 50 mM, and the corresponding shifted spectra when 50mM CPZ is added ("R+CPZ" and "B+CPZ").

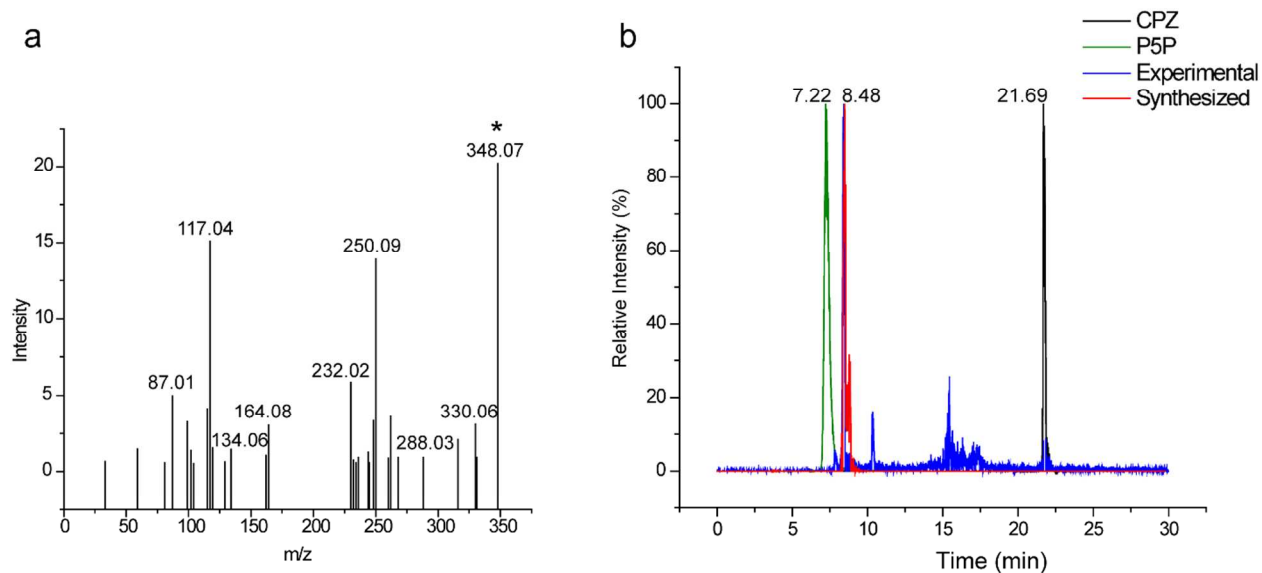


Supplementary Figure 4: MS/MS spectra of identified metabolites from MO3.13 cells. The best IDA product spectrum is chosen from all aligned cell data. Each metabolite spectrum is shown in red with the corresponding standard spectra shown above in black. All standard spectra are referenced at CE 20-30 (v) for positive mode.

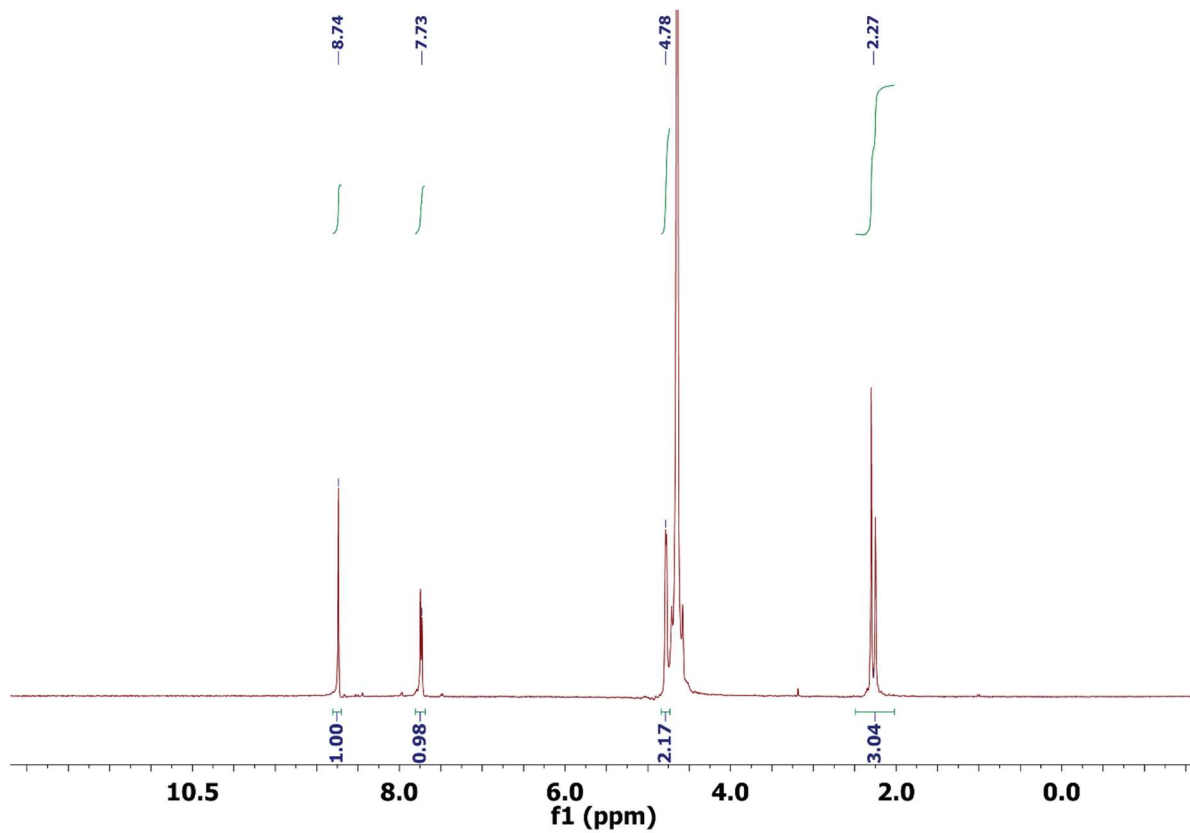




Supplementary Figure 5: MS/MS spectra of identified metabolites from mouse tissue. The best IDA product spectrum is chosen from all aligned tissue data. Each metabolite spectrum is shown in red with the corresponding standard spectra shown above in black. All standard spectra are referenced at CE 20-30 (v) for positive mode.



Supplementary Figure 6: Chemical interaction of Pyridoxal 5' Phosphate and CPZ. a) In silico fragmentation data for the proposed Schiff-base complex of P5P and CPZ. Note that many more peaks are predicted to occur using fragment-predicting algorithms than are seen with the synthesized standard. b) Total Ion Chromatograms from solutions containing CPZ (black), P5P (green), P5P with the addition of CPZ (blue) and the synthesized standard for the putative Schiff-base containing standard (red).



Supplementary Figure 7: Preparation of Schiff base from Pyridoxal-5-phosphate and oxalydihydrazide. ¹H NMR (500 MHz, D₂O with sodium bicarbonate).